ACS Photonics

Letter

pubs.acs.org/journal/apchd5

Enhanced Optical Manipulation of Cells Using Antireflection Coated Microparticles

Derek Craig,[†,‡] Alison McDonald,[†,‡] Michael Mazilu,[†] Helen Rendall,[†] Frank Gunn-Moore,[†,§] and Kishan Dholakia*[,†]

[†]SUPA and [§]School of Physics and Astronomy, University of St. Andrews, St. Andrews, Fife, United Kingdom, KY16 9SS

Supporting Information

ABSTRACT: We demonstrate the use of antireflection (AR) coated microparticles for the enhanced optical manipulation of cells. Specifically, we incubate CHO-K1, HL60, and NMuMG cell lines with AR-coated titania microparticles and subsequently performed drag force measurements using optical trapping. Direct comparisons were performed between native, polystyrene microparticle and AR microparticle tagged cells. The optical trapping efficiency was recorded by measuring the Q value in a drag force experiment. CHO-K1 cells incubated with AR microparticles show an increase in the Q value of nearly 220% versus native cells. With the inclusion of AR microparticles, cell velocities exceeding 50 μm/s were recorded for only 33 mW of laser trapping power. Cell viability was confirmed with fluorescent dyes and cells expressing a fluorescent ubiquitination-based cell cycle protein (FUCCI), which verified no disruption to the cell cycle in the presence of AR microparticles.

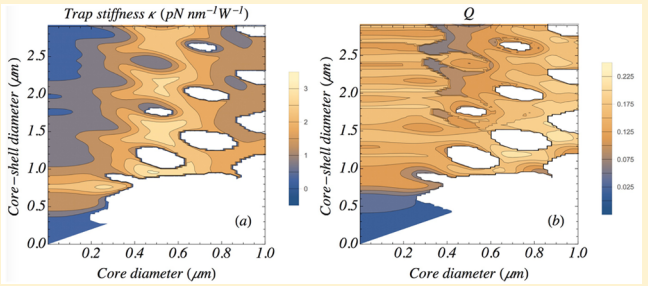

KEYWORDS: *optical trapping, dielectric tagging, antireflection, microparticles, biophotonics, cell viability*

From the first demonstration of optical manipulation of microparticles, the field has proliferated into various areas of the natural sciences.[1−3] A single beam trap in the form of optical tweezers has enabled advancement in the study of single molecule biophysics and cell microrheology.[4,5] In molecular studies, an optically trapped bead may be functionalized to attach to a specific molecule, whereas in cell studies, direct manipulation with the optical field is usually employed. Using this approach, several methods may be used to measure forces with an optical trap. However, each has its limitations and requires an accurate knowledge of the sample parameters.[6,7] In particular, force measurements can be challenging when working with nonspherical particles or in environments with an inhomogeneous viscosity, such as inside the cell. Recent developments in the field are moving toward obtaining direct force measurements by detecting light momentum changes.[8] For this approach, the calibration factor only comes from the detection instrumentation and negates the requirement to recalibrate for changes in experimental conditions.

In optical trapping, the forces generated are typically in the pN range, and efforts to maximize this have largely focused on shaping the light field to minimize aberrations.[9−11] As an alternative, recent studies have focused on enhancing the physical properties of the microparticle or trapped object itself. High refractive index microparticles hold promise for enhanced trapping due to the increased refractive index mismatch with the surrounding media. However, the resultant enhanced scattering force makes it difficult to trap these microparticles in three dimensions.[12,13]

Indeed, as a consequence of the modest dielectric contrast, that is, the minimal refractive index mismatch between a cell and its surrounding media, the optical forces for direct biological (e.g., cell) manipulation are weak.[14] Furthermore, photodamage of biological samples can occur due to prolonged exposure to a tightly focused laser spot.[15] To overcome these limitations, an optical handle, such as a silica or polystyrene microparticle, can be integrated within a cell by a process known as endocytosis or attached via the plasma membrane using a linker molecule.[16,17] Optically manipulating cells using this method is of importance for cell sorting applications.[4] Sorting of subpopulations of cells can be achieved by selectively tagging the cells of interest with a chosen microparticle. Naturally for all optical manipulations of cells maintaining a low incident laser power is essential to ensure cell viability.

Based on these considerations, we have explored the use of antireflection coated microparticles to enhance the velocity at which we can successfully transport cells, without resorting to an increase in the laser power. This could be used to develop a high throughput cell sorting system. Optically, an antireflection coating is a powerful approach to reduce deleterious reflections from a surface.[18] Recent studies have shown high refractive index anatase titania microparticles can be coated with an amorphous titania surrounding and drag force studies on such microparticles indicated forces in viscous media in excess of a nanoNewton.[18,19] However, no study has been reported using

Received: April 7, 2015
Published: September 11, 2015

DOI: 10.1021/acsphotonics.5b00178
ACS Photonics 2015, 2, 1403−1409

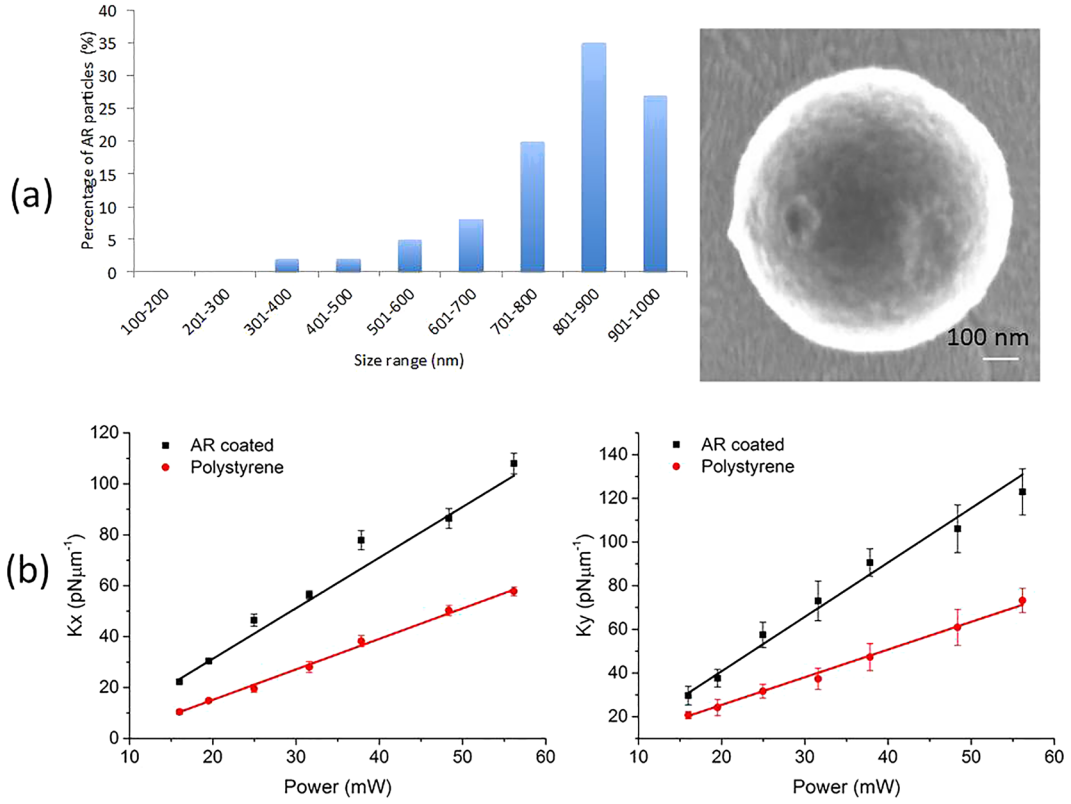

Figure 1. (a) AR microparticles with diameters sized using SEM imaging. (b) Lateral trap stiffness for both AR-coated and polystyrene microparticles as a function of trapping power for the x and y directions. Trap stiffness was determined from the corner frequency averaged over five power spectra at each power. Measurements were taken for a trapped microparticle held 5 μm above the coverslip. Data is averaged over five 800 nm polystyrene microparticles and 10 AR-coated microparticles.

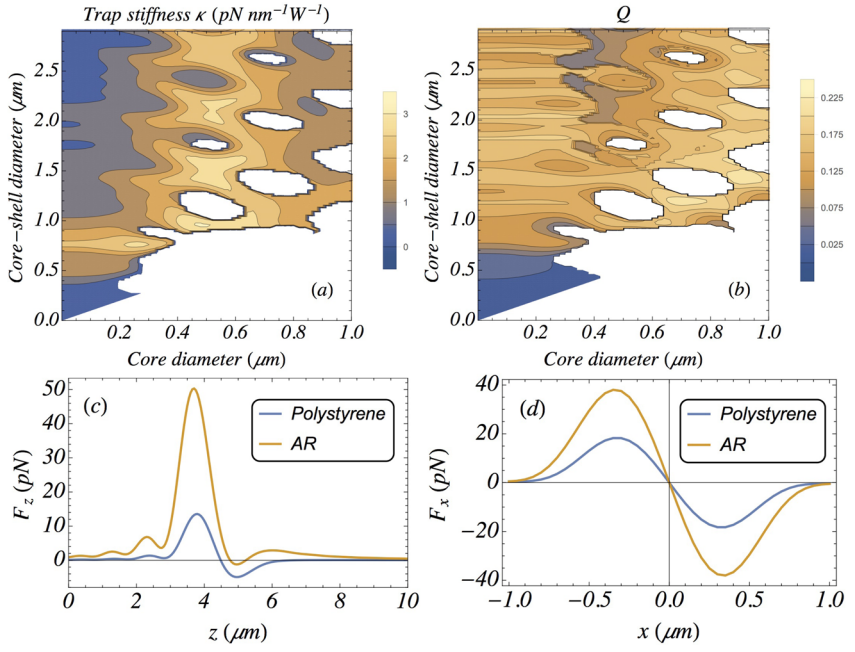

Figure 2. Numerical simulations showing enhanced trapping of AR-coated microparticles (nominally trapped 5 μm above glass slide). (a, b) Trap stiffness and Q factor enhancement as a function of the core and core−shell diameter. (c) Axial force comparison (33 mW laser power) between the AR (450 nm core and 900 nm core−shell) particle and a 800 nm polystyrene bead. (d) Same for the lateral force showing for the polystyrene bead κ = 1.25 pN nm^{-1} W^{1-} with Q = 0.058 and for the AR particle κ = 2.55 pN nm^{-1} W^{1-} with Q = 0.12.

AR microparticles in biological systems to verify their biological compatibility. Here, we address both of these issues and demonstrate the use of antireflection coated microparticles for cell trapping and manipulation.

DOI: 10.1021/acsphotonics.5b00178
ACS Photonics 2015, 2, 1403−1409

Specifically, we incubated CHO-K1, NMuMG, and HL60 cells with various concentrations of both AR-coated and polystyrene microparticles, which are internalized within these cells. The Q values measured by drag force studies indicate that AR microparticle containing cells provided a significant increase over native CHO-KI (220%) and HL60 (140%) cells, as well as an increase in comparison to a polystyrene microparticle containing CHO-KI (150%) and HL60 (115%) cells. Cell viability studies showed that cells remained healthy and were not compromised by the internalization of microparticles.

RESULTS AND DISCUSSION

As a precursor to the particle internalization studies, we characterized the lateral trap stiffness of the AR microparticles in comparison to polystyrene microparticles of a comparable size (800 nm). The trap was found to be asymmetric due to laser beam ellipticity leading to a slight difference in the x and y trap stiffness values recorded (Figure 1). The trap stiffness for the AR-coated microparticles was found to be 2.07 ± 0.06 pN·nm^{-1} W^{-1} and 2.32 ± 0.15 pN·nm^{-1} W^{-1} in the x and y directions, respectively. Whereas for polystyrene microparticles, we measured a lateral trap stiffness of 1.21 ± 0.03 pN·nm^{-1} W^{-1} and 1.30 ± 0.04 pN·nm^{-1} W^{-1}. The AR microparticles outperformed polystyrene microparticles by approximately 100%, which is comparable to results previously reported.[18] We note that batches of AR-coated microparticles exhibited a polydispersity in diameter of 20%, whereas the polydispersity reported previously was only 5%.[19] This increase in polydispersity can be attributed to differences in experimental conditions from those used in previous studies that are outwith our control. As only a narrow size regime of particles have been found to be optimized to trap at 1064 nm then the increase in polydispersity obtained is not a significant development. Previous studies on AR particles by Jannasch and Schaffer demonstrated that trapping capabilities of these particles were directly linked to the ratio between particle core size and shell thickness, with particles surrounded by thinner or thicker shells than the optimal ratio proving difficult to trap. In addition to this, problems were also encountered when attempting to trap smaller particles due to spherical aberrations at the glass−water interface.[18]

In our study, we were not able to measure the exact particle dimensions during trapping experiments. Therefore, the average AR-coated microparticle size was used in all calculations. The simulations (Figure 2) were performed using Mie scattering theory and taking into account spherical aberrations (MATLAB source code[20]). We observe that, considering the core−shell size of our particles, there is a 2- to 3-fold improvement in trap stiffness and Q value. Our results further indicate performing optical sorting of the microparticles prior to internalization experiments would be beneficial for future studies.[21] In addition, measuring the force using the state of the art full force measurements would also be advisible given the polydispersity of the sample.[22]

The Q value measurements were taken for both native AR microparticles and for polystyrene microparticles. Additionally, Q values were determined for native CHO-K1, HL60, and NMuMG cells, and finally, for cells containing internalized microparticles (see Supporting Information containing Figure S1 and Q value protocol). Average Q values were obtained using the drag force method, and the resulting Q values are presented in Table 1.

Table 1. Relative Q Value Measurements Taken Using a 1070 nm Laser-Based Single Beam Optical Trap[a]

sample	Q value (×10^{-2})	velocity (μm/s)	force range (pN)
polystyrene	2.9 ± 0.7	346−536	2.3−3.6
AR	4.2 ± 0.5	345−846	5.9−11.4
CHO-K1	1.1 ± 0.2	4.3−17.3	0.5−1.9
CHO-K1 polystyrene	1.4 ± 0.3	8.7−31.4	0.9−3.2
CHO-K1 AR	3.5 ± 0.4	16.6−56.1	1.7−5.7
HL60	1.7 ± 0.5	9.4−34.5	1.1−3.8
HL60 polystyrene	1.9 ± 0.3	10.2−40.2	0.9−3.6
HL60 AR	4.1 ± 0.3	19.6−57.2	1.8−5.1
NMuMG	1.4 ± 0.3	5−14.7	0.6−1.7
NMuMG polystyrene	1.8 ± 0.3	7−22.5	0.8−2.7
NMuMG AR	4.2 ± 0.4	6−31.3	2.0−3.6

[a]A 100× magnification oil objective (NA = 1.4) was used for all measurements. The Q value of 10 individual cells at 5 different laser powers (which were 13, 17, 22, 28, and 33 mW) was measured. The average Q value from these results is shown in the table. The velocity ranges and force ranges detailed are measurements calculated at the lowest and highest powers used in this experiment of 13 and 33 mW, respectively. The variance in Q value is the standard deviation of 10 replicate measurements.

The Q values show a significant increase in trapping efficiency of approximately 45% for AR microparticles in comparison to polystyrene microparticles. As expected, the Q values obtained for the (trypsinized) normally adherent CHO-K1 and NMuMG cells as well as the nonadherent HL60 cells, were considerably lower than those obtained for the either of the native particle solutions. This can be attributed to the weak dielectric contrast between the cells and the surrounding media. Interestingly, when drag force studies were performed on each of the cell lines following the internalization of polystyrene microparticles, only a small increase in the Q value of 10−20% was obtained. In contrast, internalization of AR microparticles increased the Q values by 220% and 140% with respect to the native cell lines. Comparison of the Q value obtained for the native AR particles in comparison to the internalized AR values shows that within statistical error there does not appear to be a loss of enhancement in trapping efficiency. We believe that a high trapping efficiency is maintained when these particles are internalized within each cell line due to the high refractive index of these particles significantly increasing the refractive index mismatch between the cells and their surrounding media. The particle tagged cell complexes shall experience a stronger gradient force due to their increased refractive index in comparison to the unlabeled cells. It is also possible to guide the particle tagged cells more rapidly than native cells due to the spheres experiencing stronger radiation pressure arising from increased scattering in the opposing direction to the propagating beam. The refractive index of the AR particles used was assumed to be between 1.7 and 1.8, which takes into account possible variations in particle shell thickness. The enhancement increase for AR particles over polystyrene particles of a similar size can also be accounted for in terms of differences in refractive index with the polystyrene particles used for comparison in this study having a refractive index of 1.5. It is worth noting that we have assumed that the cells are spherical and we have not taken into account deformations of the cell due to the hydrodynamic drag.[23] The comparative increase in Q value between the AR particle incubated adherent CHO-K1 and MNuMG cells and the suspension HL60 cells

DOI: 10.1021/acsphotonics.5b00178
ACS Photonics 2015, 2, 1403−1409

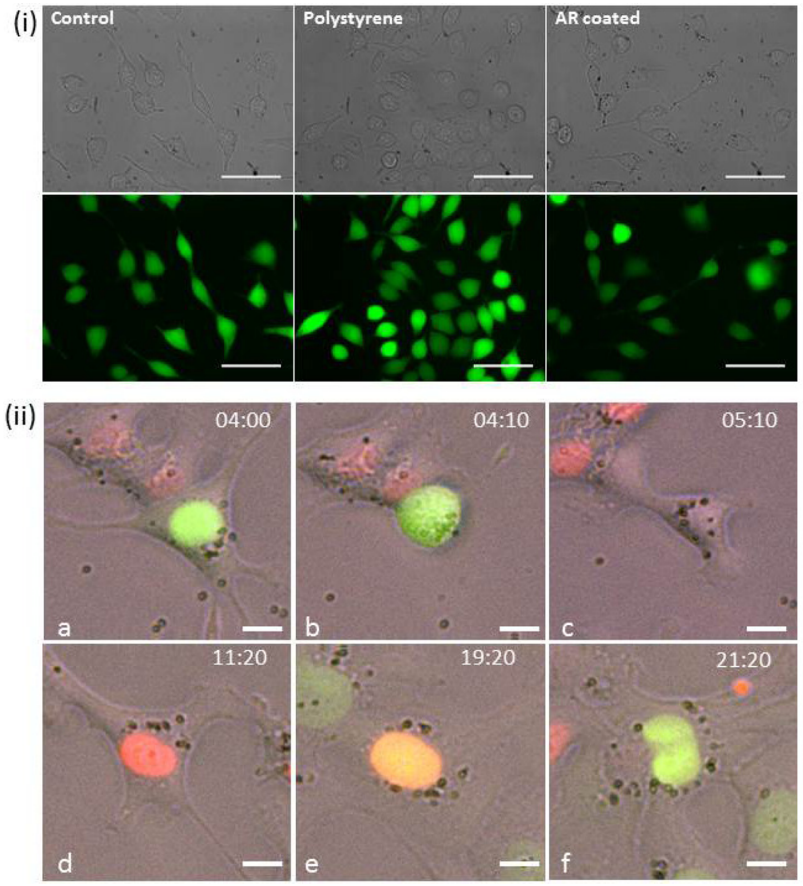

Figure 3. (i) Representative brightfield (top row) and epi-fluorescence images (bottom row) of CHO-K1 cells labeled with calcein AM. Cells imaged after a 24-h incubation with polystyrene or AR-coated microparticles are compared with a nontreated control population; 50 μm scale bar. (ii) Snapshots of FUCCI expressing cells showing successful internalization of AR microparticles. Overlay of GFP, RFP, and brightfield images taken over 24 h (images are time stamped). (a) Cell at the G2 phase, (b) M phase, (c, d) undergoing cell division G1 phase, (e) G1/S phase, and (f) S phase. These images demonstrate that the cell progressed through each cell cycle check point;[25] 10 μm scale bar.

can be attributed to the differences in the physical properties of both cell lines. When the particles are incubated with adherent cells, they will interact with the cells for a longer period of time as the particles will fall onto the surface upon which the cells are adhered to, whereas for the nonadherent cells, which are suspended freely in solution, there will be a shorter interaction time with the particles. As such, the Q value measurements for the NMuMG cells follow the same trend as the CHO-K1 cells.

To further optimize the trapping efficiency, an incubation study was performed to determine the maximum Q value possible to be obtained in comparison to the number of particles present in each cell. The particle numbers present in each cell were altered through changing the concentration of the particle solution added to the cells during the incubation process. The number of particles present in each cell was elucidated using bright field microscopy prior to Q value measurements. The corresponding data for this study is shown in Figure S1. It was deemed possible to limit the number of particles internalized within the cells to <10 through addition of a low concentration of particles during the incubation process. The resulting Q values showed a significant enhancement in favor of the AR containing cells over the polystyrene containing cells. However, as the concentration of the particle solutions was increased, it became increasingly difficult to control the number of particles entering each cell. Therefore, it was not possible to control the addition of the particles to the cells within a region of 10−20 particles. When >20 particles were present within each cell, the Q value enhancement previously gained for the AR particle containing cells was significantly reduced. This was attributed to the formation of large aggregate clusters of particles within the cell cytoplasm which we hypothesize could affect the net mass of the cells and retard their movement through solution and therefore, decrease their trapping efficiency. The localization of the particles within the cells imaged appeared to be mostly in the cytoplasmic region, although there were instances where the particles appeared to be on the membrane layer. In future studies, further functionalization of the particles with organelle targeting ligands could be a potential route to fully elucidate particle location following incubation.

Table 1 also shows the velocity and force ranges able to be exerted on the cell lines and particles. As expected, the Q values obtained for the native cell lines are significantly less than those for cells internalized with AR particles. This is reflected in the velocity and force measurements when, at the highest power of 33 mW, it was observed that the maximum velocities of 17.5 and 34.5 μm/s for the native CHO-KI and HL60 cells were obtained, respectively, with maximum forces exerted at this power on the native cells being 1.9 and 3.8 pN, respectively. In contrast, cells that had internalized <10 AR microparticles displayed a maximum velocity of 56 and 57 μm/s for the CHO-K1 and HL60 cell lines, respectively. It was possible to exert

DOI: 10.1021/acsphotonics.5b00178
ACS Photonics 2015, 2, 1403−1409

maximum forces of 5.7 and 5.1 pN, respectively. As would be expected, the forces measured for each sample increased linearly in correlation with the increasing power level. The power levels used in this study were relatively modest and reflect the power that you would wish to use to avoid compromising cell viability post optical handling. We did not perform measurements with the maximum optical power available from our system as this would compromise cell viability.

We used two fluorescence viability assays to study the biocompatibility of the microparticles over a 24 h incubation period. For the CHO-K1 and HL60 cell lines, we tested cell viability using the fluorescent stains calcein AM and propidium iodide.[24] With respect to calcein AM, live cells exhibit uniform fluorescence staining of the cytoplasm after acetoxymethyl ester hydrolysis by intracellular esterases.[24] Nonviable cells were identified by punctate calcein AM staining or by fluorescence of propidium iodide within the nuclear region. We found >90% cell viability between the untreated cells and those treated with AR-coated or polystyrene microparticles for both cell lines. Representative images of viable CH0-K1 cells are shown in Figure 3. To further study the effect of particle internalization on the development of the cells in culture, we performed timelapse imaging on NMuMG cells, which express the FUCCI fluorescent assay system. A series of images from a time-lapse study with AR-coated microparticles showing the life cycle of one cell and its daughter cell are shown in Figure 3. We found no significant variation between the life cycle of control cells and cells containing microparticles. Additionally, microparticles were shown to be transported around the cytoplasm of the cell and were successfully distributed between the daughter cells. It should be noted that the cell viability studies described were performed in order to determine that the cells remained viable pre- and postincubation with the AR and polystyrene particles and not pre- and postoptical trapping.

Parameters such as laser power and exposure time have to be carefully considered to ensure that cell viability is not compromised after trapping experiments. Furthermore, studies have investigated the further growth of CHO-K1 cells postoptical trapping with one study reporting that trapping with a 1064 nm laser source significantly reduced the cloning efficiency of CHO-K1 cells to <40% after 5 min exposure with >80 mW power.[26] Our approach of enhancing the dielectric contrast between the cells and the surrounding media allows for manipulation of cells using a significantly lower power. Using AR-coated microparticles provides the means to reduce this further. Combined with the proven biocompatibility of these microparticles, our study shows great promise of enhanced optical handling without compromising the viability of the cells.

CONCLUSION

We have demonstrated the first application of antireflection coated particles for enhanced cell manipulation. Our study details the first direct comparison between polystyrene particles and antireflection-coated particles for the indirect optical manipulation of cells via optical tagging. Significant increases in trapping efficiency were obtained when AR tagged cells were compared to both polystyrene tagged and native cell lines. We have also proven that cell viability is not compromised during the internalization of these AR microparticles. Future applications of this technique could include further particle functionalization to target specific cell sub populations for subsequent cell sorting or for enhanced force measurements inside living cells. The ability to use lower laser powers to optically manipulate cells containing antireflection-coated particles should allow for faster optical manipulation during cell sorting experiments without inducing irreversible cell damage. The use of these particles could also be used for other indirect optical manipulation studies such as single molecular studies of DNA and RNA, the manipulation and stretching of cells such as red blood cells, and further studies of molecular interactions. In the studies listed previously, there has been a persistent need to use an increasing number of optical handles in order to exert increased forces on these objects, whereas, with the advent of these AR particles, it could be possible to exert these forces not only on a smaller number of particles but at significantly less laser power than previously required.

METHODS

AR Microparticle Synthesis and Characterization. Synthesis of AR microparticles was successfully achieved using a combination of two methods.[18,19] Briefly, 0.23 g of titanium butoxide is mixed with anhydrous ethylene glycol then added to a 100 mL of acetone containing 0.24 g of Tween-20. Following sedimentation overnight and purification by centrifugation, the obtained seeds were calcined at 500 °C for 2 h. The resulting anatase seeds were resuspended in 10 mL of ethanol prior to adding a further 10 mL of ethanol containing 0.14 g of titanium butoxide. The combined solution was sonicated for 2 h, prior to purification by centrifugation. The microparticles were then dried at 50 °C for 2 h. We used SEM imaging to measure the diameter of the particles before and after coating to find the mean core diameter as well as the final diameter postcoating.

Cell Culture and Particle Incubation. We cultured three cell lines, two adherent and one nonadherent, for particle incubation and trapping experiments. All cell lines were cultured in a 37 °C, 5% CO_2 humidified incubator. The adherent chinese hamster ovary (CHO-K1) and mouse mammary gland (NMuMG) cell lines were grown in Minimum Eagles medium (SIGMA) supplemented with 10% (v/v) fetal bovine serum, 2 mM L-glutamine, and 1% penicillin−streptomycin and 0.5 mg/mL Geneticin. Cells were plated onto plastic bottom Petri dishes for particle incubation experiments and allowed to grow for 24 h before adding each particle set. Following the addition of both AR and polystyrene microparticles to the cells, they were incubated for a further 24 h prior to trypsinization and resuspension in fresh prewarmed media. Nonadherent human promyelocytic leukemia cells (HL60) were grown in RPMI-1640 media (SIGMA), supplemented as above. As this was a suspension culture, we did not have to plate out cells 24 h before adding particles. The microparticle incubation procedure was the same as described for the adherent cell lines.

Cell Viability Assays. We performed two cell viability assays following the 24 h microparticle incubation. The first assay used calcein AM and propidium iodide fluorescent labeling. We used this method to test the viability for the CHO-K1 and HL60 cell lines. The cells where incubated with 3 μM propidium iodide and 2 μM calcein AM solutions in 1× phosphate buffered saline. We visualized the cells using epi-fluorescence imaging with FITC and TRITC filter cubes. The number of live and dead cells were counted over a population of 500 cells per dish, and the experiments were conducted in triplicate. The NMuMG cell line used in these experiments had been previously transfected with the FUCCI constructs and

DOI: 10.1021/acsphotonics.5b00178
ACS Photonics 2015, 2, 1403−1409

cryo-preserved.[25] Using time-lapse epi-fluorescence microscopy, we were able to image the stage in the life cycle for each cell and could track the progression on a single cell basis. We studied the cell development with and without microparticles present. We conducted these experiments in triplicate and due to the limited field of view we were only able to track the development of on average 10 cells per dish. Cells were maintained in a microscope stage top incubator, 37 °C, 5% CO_2, for the 24 h imaging period. Fluorescence and brightfield images were taken at 5 min intervals.

Preparation of Cells for Trapping Experiments. All cells to be analyzed in drag force measurements were placed onto BSA (3% w/v) coated glass dishes (Fluorodish, World Precision Instruments). The size of the cell was measured from the brightfield image and noted prior to trapping. The measured cell diameters were in the range of 11.8−17.3 μm for CHO-K1, 12.1−15.0 μm for NMuMG, and 12.8−17.4 μm for the HL60 cells. The number of internalized microparticles was counted in each trapped cell using bright-field microscopy. Cells were then broadly categorized into three cohorts (<10, 10−20, and >20 internalized microparticles).

Optical Trapping System. The optical trap was built around a commercial inverted microscope (Nikon, Eclipse Ti) and used a continuous-wave Ytterbium fiber laser emitting at 1070 nm (10 W maximum power). The laser was operated at a fixed current well above threshold. The power available for the optical trap was controlled using a combination of a half-wave plate and polarizing beam splitter (PBS) cube. The laser beam was expanded to overfill the back aperture of the objective lens, resulting in a diffraction limited focal spot. We used a 60×/1.4 NA oil immersion objective lens with a measured optical transmission of 39% for trap stiffness measurements and a 100×/1.4 NA oil objective for Q value measurements (transmission of 30%). The optical power at the trapping plane was accurately determined from the measured power at the back aperture and the transmission of the objective lens.

Trap stiffness measurements were performed using back focal plane (BFP) interferometry in transmission mode by imaging the BFP of a detection objective onto a quadrant photodiode (QPD). This allowed tracking in the time domain of the position of the trapped microparticle. Data was acquired at 50 kHz sampling frequency over 10 s and saved using custom LabVIEW software (Elliot Scientific). The data was analyzed using the power spectrum method to obtain the corner frequency using freely available MATLAB code.[27] Measurements were taken at varying power to measure the linear power dependence on the lateral trap stiffness for both AR-coated and polystyrene microparticles. We estimated the linear region of the trap to be 170 nm. The height of the trap above the coverslip was measured relative to a fixed point on the coverslip surface. For drag force measurements, we used a motorized stage (Märzhäuser Wetzlar) to control the translation speed of the sample relative to the stationary beam.

Optical Trapping Model. We have modeled the optical forces acting on coated and uncoated microparticle using a Mie scattering approach. The Mie coefficients were calculated using the MATLAB MatScat package[28] and spherical aberration was implemented using an angular spectral decomposition approach.[29] The optical force calculation only took into account the optical eigenmodes of the system[30,31] and were performed using the MATLAB EigenOptics package.[20]

***Q* Value Measurement Protocol.** The trap efficiency was determined by the established by drag force approach to determine the Q value for each cell/microparticle in question.[32] Solutions of each set of particle were freshly prepared prior to each set experiments by resuspending the microparticles in a solution of Milli-Q water at a concentration of 1 mg/mL. Dilutions were then made from each stock solution accordingly. Solutions of AR and polystyrene microparticles at 25% and 37.5% of the original stock concentration respectively, were incubated with each cell line for 24 h.

■ ASSOCIATED CONTENT

Supporting Information

The Supporting Information is available free of charge on the ACS Publications website at DOI: 10.1021/acsphotonics.5b00178.

Raw data and simulation data are available online.[33] The numerical model is available online.[20] Supplementary figure, Figure S1 is included (PDF).

■ AUTHOR INFORMATION

Corresponding Author

*E-mail: kd1@st-andrews.ac.uk.

Author Contributions

‡These authors contributed equally to this work (D.C. and A.M.).

Notes

The authors declare no competing financial interest.

■ ACKNOWLEDGMENTS

We thank the UK Engineering and Physical Sciences Research Council under Grants EP/J01771X/1 and EP/M000869/1, the University of St Andrews, the BRAINS 600th anniversary appeal, and Dr. Killick for funding. We thank Professor David Cole-Hamilton for advice on AR particle synthesis.

■ REFERENCES

(1) Ashkin, A. Acceleration and Trapping of Particles by Radiation Pressure. *Phys. Rev. Lett.* **1970**, *24*, 156−159.

(2) Perkins, T. T. Angstrom-Precision Optical Traps and Applications. *Annu. Rev. Biophys.* **2014**, *43*, 279−302.

(3) Dholakia, K.; Cizmar, T. Shaping the future of manipulation. *Nat. Photonics* **2011**, *5*, 335−342.

(4) Mthunzi, P.; Lee, W. M.; Riches, A. C.; Brown, C. T. A.; Gunn-Moore, F. J.; Dholakia, K. Intracellular Dielectric Tagging for Improved Optical Manipulation of Mammalian Cells. *IEEE J. Sel. Top. Quantum Electron.* **2010**, *16*, 608−618.

(5) Block, S. M.; Goldstein, L. S. B.; Schnapp, B. J. Bead movement by single kinesin molecules studied with optical tweezers. *Nature* **1990**, *348*, 348−352.

(6) Neuman, K. C.; Block, S. M. Optical trapping. *Rev. Sci. Instrum.* **2004**, *75*, 2787−2809.

(7) Perkins, T. T. Optical traps for single molecule biophysics: a primer. *Laser Photonics Rev.* **2009**, *31*, 203−220.

(8) Farre, A.; Montes-Usategui, M. A force detection technique for single-beam optical traps based on direct measurement of light momentum changes. *Opt. Express* **2010**, *11*, 11955−11968.

(9) Neuman, K. C.; Nagy, A. Single-molecule force spectroscopy: optical tweezers, magnetic tweezers and atomic force microscopy. *Nat. Methods* **2008**, *5*, 491−505.

(10) Wulff, K. D.; Cole, D. G.; Clark, R. L.; DiLeonardo, R.; Leach, J.; Cooper, J.; Gibson, G.; Padgett, M. J. Aberration correction in holographic optical tweezers. *Opt. Express* **2006**, *14*, 4170−4175.

(11) Cizmar, T.; Mazilu, M.; Dholakia, K. In situ wavefront correction and its application to micromanipulation. *Nat. Photonics* **2010**, *4*, 388−394.

DOI: 10.1021/acsphotonics.5b00178
ACS Photonics 2015, 2, 1403−1409

(12) Hu, Y.; Nieminen, T. A.; Heckenberg, N. R.; Rubinsztein-Dunlop, H. Antireflection coating for improved optical trapping. *J. Appl. Phys.* **2008**, *103*, 093119.
(13) van der Horst, A.; van Oostrum, P. D. J.; Moroz, A.; van Blaaderen, A.; Dogterom, M. High trapping forces for high-refractive index particles trapped in dynamic arrays of counterpropagating optical tweezers. *Appl. Opt.* **2008**, *47*, 3196−3202.
(14) Wang, M. M.; Tu, E.; Raymond, D. E.; Yang, J. M.; Zhang, H. C.; Hagen, N.; Dees, B.; Mercer, E. M.; Forster, A. H.; Kariv, I.; Marchand, P. J.; Butler, W. F. Microfluidic sorting of mammalian cells by optical force switching. *Nat. Biotechnol.* **2005**, *23*, 83−87.
(15) Neuman, K. C.; Chadd, E. H.; Liou, G. F.; Bergman, K.; Block, S. M. Characterization of photodamage to Escherichia coli in optical traps. *Biophys. J.* **1999**, *77*, 2856−2863.
(16) Ozkan, M.; Wang, M.; Ozkan, C.; Flynn, R.; Birkbeck, A.; Esener, S. Optical manipulation of objects and biological cells in microfluidic devices. *Biomed. Microdevices* **2003**, *5*, 61−67.
(17) Rabinovitch, M. Professional and nonprofessional phagocytes - an introduction. *Trends Cell Biol.* **1995**, *5*, 85−87.
(18) Jannasch, A.; Demirors, A. F.; van Oostrum, P. D. J.; van Blaaderen, A.; Schaffer, E. Nanonewton optical force trap employing anti-reflection coated, high-refractive-index titania microspheres. *Nat. Photonics* **2012**, *6*, 469−473.
(19) Demirörs, A. F.; Jannasch, A.; van Oostrum, P. D. J.; Schäffer, E.; Imhof, A.; van Blaaderen, A. Seeded Growth of Titania Colloids with Refractive Index Tunability and Fluorophore Free Luminescence. *Langmuir* **2011**, *27*, 1626−1634.
(20) Mazilu, M. *EigenOptics* (online); University of St. Andrews, St. Andrews, U.K., 2015; DOI: 10.17630/f039c29b-12fe-4b4b-9b0b-907c72634ad8 (accessed July 2, 2015).
(21) MacDonald, M.; Spalding, G.; Dholakia, K. Microfluidic sorting in an optical lattice. *Nature* **2003**, *426*, 421−424.
(22) Farre, A.; Marsa, F.; Montes-Usategui, M. Optimized back-focal-plane interferometry directly measures forces of optically trapped particles. *Opt. Express* **2012**, *20*, 12270−12291.
(23) Foo, J. J.; Liu, K. K.; Chan, V. Viscous drag of deformed vesicles in optical trap: Experiments and simulations. *AIChE J.* **2004**, *50*, 249−254.
(24) Antkowiak, M.; Torres-Mapa, M. L.; Gunn-Moore, F.; Dholakia, K. Application of dynamic diffractive optics for enhanced femtosecond laser based cell transfection. *J. Biophotonics* **2010**, *3*, 696−705.
(25) Sakaue-Sawano, A.; Kurokawa, H.; Morimura, T.; Hanyu, A.; Hama, H.; Osawa, H.; Kashiwagi, S.; Fukami, K.; Miyata, T.; Miyoshi, H.; Imamura, T.; Ogawa, M.; Masai, H.; Miyawaki, A. Visualizing Spatiotemporal Dynamics of Multicellular Cell-Cycle Progression. *Cell* **2008**, *132*, 487−498.
(26) Liang, H.; Vu, K. T.; Krishnan, P.; Trang, T. C.; Shin, D.; Kimel, S.; Berns, M. W. Wavelength dependence of cell cloning efficiency after optical trapping. *Biophys. J.* **1996**, *70*, 1529−1533.
(27) Tolić-Nørrelykke, I. M.; Berg-Sørensen, K.; Flyvbjerg, H. MatLab program for precision calibration of optical tweezers. *Comput. Phys. Commun.* **2004**, *159*, 225−240.
(28) Schäfer, J.-P. Implementierung und Anwendung analytischer und numerischer Verfahren zur Lösung der Maxwellgleichungen für die Untersuchung der Lichtausbreitung in biologischem Gewebe. *Ph.D. thesis*, Universität Ulm. Fakultät für Naturwissenschaften: Ulm, Germany, 2011.
(29) Ranha Neves, A. A.; Fontes, A.; Cesar, C. L.; Camposeo, A.; Cingolani, R.; Pisignano, D. Axial optical trapping efficiency through a dielectric interface. *Phys. Rev. E* **2007**, *76*, 061917.
(30) Baumgartl, J.; Kosmeier, S.; Mazilu, M.; Rogers, E. T. F.; Zheludev, N. I.; Dholakia, K. Far field subwavelength focusing using optical eigenmodes. *Appl. Phys. Lett.* **2011**, *98*, 181109.
(31) De Luca, A. C.; Kosmeier, S.; Dholakia, K.; Mazilu, M. Optical eigenmode imaging. *Phys. Rev. A: At., Mol., Opt. Phys.* **2011**, *84*, 021803(R).
(32) Lee, W. M.; Reece, P. J.; Marchington, R. F.; Metzger, N. K.; Dholakia, K. Construction and calibration of an optical trap on a fluorescence optical microscope. *Nat. Protoc.* **2007**, *2*, 3226−3238.
(33) Craig, D.; McDonald, A.; Mazilu, M.; Rendall, H. A.; Gunn-Moore, F. J.; Dholakia, K. *Data Underpinning: Enhanced Optical Manipulation of Cells Using Anti-Reflection Coated Microparticles*; University of St. Andrews: St. Andrews, U.K., 2015; DOI: 10.17630/6b2cc9f9-90f2-4b83-9990-35cff3ff31e5 (accessed July 2, 2015).

DOI: 10.1021/acsphotonics.5b00178
ACS Photonics 2015, 2, 1403−1409